

# Reagent integration and controlled release for multiplexed nucleic acid testing in disposable thermoplastic 2D microwell arrays

Cite as: Biomicrofluidics 15, 014103 (2021); doi: 10.1063/5.0039146

Submitted: 30 November 2020 · Accepted: 5 January 2021 ·

Published Online: 15 January 2021



View Online



Export Citation



CrossMark

S. Padmanabhan,<sup>1</sup> A. Sposito,<sup>2</sup> M. Yeh,<sup>2</sup> M. Everitt,<sup>3</sup> I. White,<sup>3</sup> and D. L. DeVoe<sup>1,2,3,a</sup>

## AFFILIATIONS

<sup>1</sup> Department of Chemical and Biomolecular Engineering, University of Maryland, College Park, Maryland 20742, USA

<sup>2</sup> Department of Mechanical Engineering, University of Maryland, College Park, Maryland 20742, USA

<sup>3</sup> Department of Bioengineering, University of Maryland, College Park, Maryland 20742, USA

<sup>a</sup>Author to whom correspondence should be addressed: ddev@umd.edu. Tel.: +1-301-405-8125.

## ABSTRACT

The seamless integration of reagents into microfluidic devices can serve to significantly reduce assay complexity and cost for disposable diagnostics. In this work, the integration of multiplexed reagents into thermoplastic 2D microwell arrays is demonstrated using a scalable pin spotting technique. Using a simple and low-cost narrow-bore capillary spotting pin, high resolution deposition of concentrated reagents within the arrays of enclosed nanoliter-scale wells is achieved. The pin spotting method is further employed to encapsulate the deposited reagents with a chemically modified wax layer that serves to prevent disruption of the dried assay components during sample introduction through a shared microchannel, while also enabling temperature-controlled release after sample filling is complete. This approach supports the arbitrary patterning and release of different reagents within individual wells without crosstalk for multiplexed analyses. The performance of the in-well spotting technique is characterized using on-chip rolling circle amplification to evaluate its potential for nucleic acid-based diagnostics.

Published under license by AIP Publishing. <https://doi.org/10.1063/5.0039146>

## I. INTRODUCTION

There is a large and growing need for near-patient and point-of-care diagnostics to improve access and reduce costs for early detection of disease biomarkers to ensure appropriate, timely, and cost-effective treatment. To this end, microfluidic technologies have long been recognized as a powerful tool, with advantages including low sample volume consumption, rapid turnaround time, low cost, and portability that can be leveraged for effective point-of-care testing.<sup>1–4</sup> Additionally, due to their capabilities for isolating multiple independent reaction volumes within a single device, microfluidic technologies also offer potential for multiplexed point-of-care testing, wherein multiple biomarkers can be screened simultaneously within a single patient sample to support assays that require analysis of more than a single molecular target, and reduce the cost and time required for comprehensive profiling of multiple disease states.<sup>5,6</sup>

At the macroscale, multiplexed assays are commonly performed using conventional well plates to segregate reactions, with

manual or robotic pipetting to deliver selected reagents and sample to the wells prior to test execution. While this approach offers flexible assay design and implementation, it is not suitable for point-of-care diagnostics where ease of use is paramount. To minimize the number of assay steps required for microfluidic diagnostics, all reagents required for assay operation should ideally be integrated during chip manufacture, thereby simplifying device operation, reducing the need for external instrumentation, lowering the risk of cross contamination, and enhancing overall system portability.<sup>7</sup> Various approaches to microfluidic reagent integration have been explored, with assay components integrated on-chip either in liquid form<sup>7,8</sup> using blisters<sup>9</sup> and ampoules<sup>10</sup> or in solid form<sup>7</sup> as dried,<sup>11–15</sup> lyophilized,<sup>16,17</sup> and gelified<sup>18–20</sup> reagents. While on-chip liquid and solid storage have both garnered significant commercial interest,<sup>21</sup> dried reagent storage offers a number of advantages including improved long-term stability and the ability to reconstitute the dried reagents upon sample introduction within the need for any mechanical operations such as breaking a

seal to release liquid-phase solutions. While assay components can be deposited into a microfluidic substrate using a manual pipette for large-volume storage,<sup>13</sup> more precise deposition techniques are required as storage chamber dimensions are reduced below the millimeter size scale. In particular, both contact and non-contact printing methods<sup>22,23</sup> can be used to ensure precise integration with high resolution without the risk of cross contamination.<sup>7</sup> A variety of high-throughput non-contact printing techniques have been developed for microarray fabrication, including laser printing,<sup>22–24</sup> photochemical printing,<sup>22,25–27</sup> inkjet printing,<sup>22,23,28–31</sup> and electrospray deposition.<sup>22,32,33</sup> While these methods can provide high precision and throughput, they have certain limitations. In the case of inkjet printing, the process of switching reagents within a printer head involving washing steps could be time consuming and cumbersome,<sup>34</sup> and the large-volume requirements for typical print head reservoirs precludes their use when depositing highly limited solutions. Also, the possibility of satellite drop formation and splashing could lead to the risk of cross contamination during inkjet printing of reagents.<sup>30</sup> Another limitation involves a potential risk of denaturing deposited biomolecules in the case of inkjet printing,<sup>35</sup> electrospray deposition, and photochemical printing.<sup>22,26</sup> A further limitation of the latter methods is that they place constraints on the reagent solution properties such as fluid viscosity, as well as substrate conditions that may prohibit their use for some applications.

In contrast to these non-contact printing methods, contact printing involves direct mechanical interfacing between the liquid reagent source and target substrate during reagent deposition.<sup>22,23</sup> Contact printing can provide uniform spotting volumes using a simple workflow that requires minimal maintenance,<sup>22,36</sup> using a serial process such as pin printing<sup>37,38</sup> or a parallel process based on microstamping.<sup>22,23,38–41</sup> Microstamping, commonly performed using patterned PDMS (polydimethylsiloxane) stamps,<sup>42,43</sup> allows parallel deposition of multiple spots with exceptionally high resolution,<sup>40</sup> but severely limits the reagent volumes that can be transferred, and suffers from non-specific adsorption of reagents on the stamp surface that can limit their reuse.<sup>22</sup>

Comparatively, pin spotting is a flexible and widely used technique that offers a simple, reproducible, and reliable approach for uniform patterning of microarrays. While pin spotting is a serial process, it is readily automated using simple robotics for high spatial control and is capable of transferring a wide range of reagent compositions and volumes. Pin spotting is typically performed using either solid or split tip pins,<sup>38</sup> with reagent uptake at the pin tip due to surface tension and capillary action, followed by transfer and deposition onto the target substrate. Solid pins are generally used for low density spotting and for depositing viscous reagents that can otherwise clog narrow capillaries and offer the benefit of easy cleaning after use.<sup>22</sup> Alternatively, split pins have narrow capillaries within the tip that serve as reagent reservoirs enabling higher throughput spotting of picoliter to nanoliter volumes, as typically required for nucleic acid microarray applications. In both cases, commercial pins that are designed for deposition onto a planar substrate possess conical tips with millimeter-scale outer diameters that can hinder the deposition of reagents inside small patterned substrates such as microchannels and sub-microliter sample wells. Various microfluidic-enabled

deposition tips have also been reported, allowing for the metering of solutions from integrated microchannels onto off-chip substrates. This integrated approach can enable functionality beyond simple reagent transfer, such as precise control over bidirectional flow<sup>44</sup> and parallel multi-tip arrays,<sup>45,46</sup> although at the cost of higher fabrication and system complexity.

Here, we employ a simple and low-cost capillary spotting pin fabricated from a stainless-steel blunt-tip dispensing needle to overcome the limitations of commercial pins for microfluidic reagent packaging and demonstrate its use for multiplexed reagent integration (Fig. 1). The capillary needle offers a sub-millimeter cylindrical tip that allows for contact spotting within microwells with volumes on the order of tens to hundreds of picoliters. When combined with a robotic stage for precise position control, the resulting spotting tips provide an effective approach to depositing liquid reagent solutions into on-chip microwells followed by drying or lyophilization to enable long-term storage.

The custom spotting pins are also used to enable controlled thermo-responsive reagent release. Following the deposition of discrete reagent volumes within a microfluidic substrate, the dried reagents must be protected from dissolution during aqueous sample introduction to prevent dispersion and mixing between isolated reaction volumes. This can be achieved using an appropriate encapsulant for the dried reagents to inhibit or slow water infiltration. For large-volume reagent storage, sugars such as sucrose and trehalose are often used to delay the dissolution of underlying reagents, while also providing the benefit of stabilizing macromolecules such as polymerases for long-term storage.<sup>7,47</sup> However, sugar encapsulation is not suitable for use in nanoliter-scale wells due to its high dissolution rate. An alternative approach is to use an encapsulant that enables active control over the release process through a user-defined change in temperature or pH to provide on-demand release.<sup>7</sup> Paraffin wax is a commonly used encapsulant that is compatible with nucleic acid amplification techniques such as polymerase chain reaction (PCR) and has been previously employed for temperature-controlled release in microfluidic devices employing millimeter-scale chambers with manually deposited reagents.<sup>11–13</sup> In these examples, paraffin wax encapsulation was

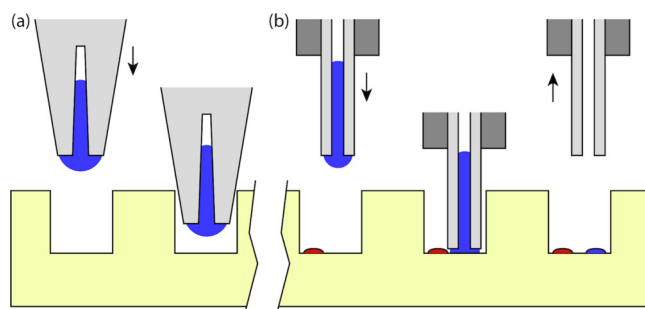


**FIG. 1.** Microwell reagent integration by contact spotting. (a) Conventional tapered spotting pins are too large to deposit reagents into picoliter-scale wells. (b) Sub-millimeter cylindrical capillary pins allow multiple discrete spots to be deposited within individual wells.

achieved by manually depositing large volumes of wax shavings<sup>11</sup> or molten wax<sup>12</sup> inside large ( $>10\mu\text{l}$ ) reaction chambers. As the reaction chamber volume is reduced, these deposition techniques are no longer suitable since tighter control over the volume and final thickness of the encapsulation layer is required. Here, we extend the pin spotting technique as a highly controllable method for automated encapsulation of pre-deposited reagents within sub-millimeter microwells. Because the paraffin layer is hydrophobic, the presence of wax can prevent the sample from entering smaller wells where a low water contact angle on the well surfaces is critical for reliable filling,<sup>48</sup> resulting in low and variable sample volumes or trapped air bubbles that degrade assay performance. To address this issue, a strategy for chemically modifying the wax layer to render it hydrophilic is presented, enabling highly efficient and repeatable filling of the wells during sample introduction. The overall reagent deposition and encapsulation process is optimized for an enclosed 2D micowell array patterned in a thermoplastic microfluidic chip sealed by solvent bonding, and the functionality of resulting devices is studied through the implementation of a rolling circle amplification (RCA) reaction using integrating reagents and hydrophilic-modified paraffin for controlled release, with variable reagent amounts deposited within different wells to investigate the impact of reagent concentration on amplification efficiency.

## II. MATERIALS AND METHODS

### A. Microfluidic device fabrication

Thermoplastic microfluidic devices containing 2D arrays of cubic microwells with side dimensions ranging from 400 to  $800\mu\text{m}$  and prismatic microwells with side dimensions of 1.5 mm and depth of  $800\mu\text{m}$  were fabricated in 2 mm thick cyclic olefin polymer (COP) plates (Zeonor 1020R, Zeon Chemicals, Louisville, KY) by direct milling using a three-axis CNC milling machine (MDX650, Roland DGA, Irvine, CA). The resulting microwells were solvent polished using cyclohexane vapor for minimizing surface roughness.<sup>48</sup> Solvent polishing was performed by mounting the micowell substrate on a glass plate with Scotch tape (3M, Maplewood, MN) and placing the plate on the top of a glass dish (12.7 cm diameter, 15.2 cm height) containing cyclohexane poured to a height of 5 mm. The sealed dish was held at 30 °C for 10 min, followed by degassing of the micowell substrate in a vacuum oven at 40 °C for 2 h. This was followed by hydrophilic surface modification of the micowell substrate by surfactant adsorption.<sup>48</sup> The microwells were sonicated after 55 s oxygen plasma exposure in a 20 mg/ml solution of the hydrophilic triblock copolymer Pluronic F-108 (Sigma Aldrich, St. Louis, MO) in DI water for 1 h, followed by nitrogen drying and baking at 60 °C for 1 h to remove the excess solution. Reagents were deposited into each micowell by pin spotting before sealing the chip with a second COP substrate containing a single wide microchannel (400  $\mu\text{m}$  deep) spanning the full width of the micowell array, with milled holes (635  $\mu\text{m}$  diameter) providing fluidic access to each end of the channel. To prevent melting or dissolution of the paraffin encapsulant layer, chip sealing was performed using a modified room temperature solvent bonding process,<sup>48</sup> involving the immersion of the capping microchannel layer in a 35% (w/w) solution of

decahydronaphthalene (Thermo Fisher Scientific, Rockford, IL) in ethanol for 5.5 min, followed by rinsing in ethanol and drying with nitrogen. The capping microchannel layer was aligned to the microwell layer containing the deposited reagents, and the assembly was placed in a laminator (PL-1200HP Roll Laminator, Professional Laminating System, Hamilton, MT) at a low roller speed, followed by placing the assembly in a hot press (AutoFour/15, Carver Inc., Wabash, IN) and applying a 200 lb load at 22 °C for 5 min. The chip was then degassed under vacuum at room temperature for 15 min to remove residual solvent prior to testing.

### B. Pin spotting

Pin spotting inside the 2D micowell arrays was carried out using a custom tool and spotting pins. The tool comprised three linear actuators (LS1-6-C125-EH-PNP-3-X, Deltron Precision Inc, Bethel, CT) driven by stepper motors (LV141-02-10, Parker Hannifin Corp., Cleveland, OH) and a motor driver (ED-Drive, Parker Hannifin) to enable precise positioning in X, Y, and Z axis. Two photoelectric sensors (PM-Y54P, Panasonic, Newark, NJ) were used as limit switches on each axis to control the travel distance and calibrate the origin coordinates during the tool homing cycle. The entire system was controlled using an Arduino microcontroller (Adafruit, New York, NY) along with an open source motion control software (GRBL) for interfacing using G-code to specify motion paths. Two thermoelectric heaters were positioned on the fixed stage for reagent drying and wax heating.

The spotting pin used for reagent and wax deposition was fabricated from a 0.5 in. long blunt-tip stainless-steel dispensing needle (60  $\mu\text{m}$  i.d. and 250  $\mu\text{m}$  o.d.) with a supporting structure designed to allow the pin to fit into a commercial spotting head as shown in Fig. 2. To make the pin, a stainless-steel tube segment (0.21 cm o.d.) was cut to 6.1 cm length and capped with a nylon washer that serves to maintain the vertical position of the pin within its holder. A PEEK sleeve was inserted into the tube, and the stainless-steel needle was inserted inside the PEEK sleeve. The inner and outer diameters of the components were selected to allow for a simple press fit, with a small volume of an epoxy adhesive applied to the mating for permanent assembly. Because the bore of the assembly is hollow, top cleaning is easily performed by

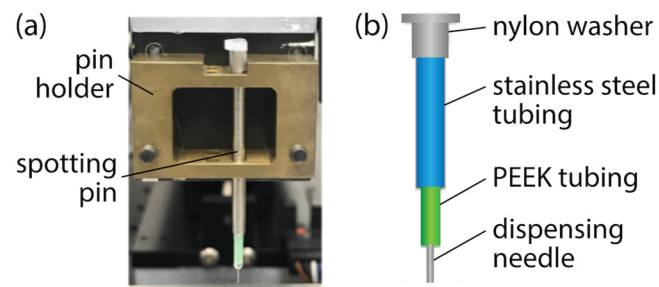


**FIG. 2.** (a) Photograph of a spotting pin mounted in the holder. (b) Schematic of the custom cylindrical spotting pin.

perfusing solvent through the center of the nylon washer. The final cost of the pin was below \$5.

For reagent deposition, a small volume of reagent is aspirated into the needle tip by capillary action. The aspirated reagent volume is then used to deposit multiple uniform picoliter spots on the substrate. Reagent spotting was performed with selected reagents added to a spotting buffer consisting of 20% (w/w) polyethylene glycol (PEG) (average MW 20 kDa, 81300, Sigma Aldrich, St. Louis, MO), 10% (v/v) glycerol (Sigma Aldrich), and 0.1% (v/v) tritonX-100 surfactant (Sigma Aldrich). During reagent deposition, the spotting pin approached the bottom of the microwell substrate at a rate of 1.67 mm/s before touching the substrate for a dwell time of 0.5 s before retracting at 1.67 mm/s. After spotting, the reagents were dried at 41 °C for 5 min before wax deposition for encapsulation. When changing spotting solutions, the hollow pin was flushed with DI water and dried with nitrogen to prevent carry-over between deposition cycles.

Wax spotting was performed using the same spotting tip design employed for reagent deposition. However, rather than retaining fluid within the needle for successive deposition events, the needle was dipped in the wax bath before each encapsulant spotting step. The wax composition consisted of white petrolatum (Vaseline, Unilever, USA) with the addition of 1% Span 20 (v/v) (Sigma Aldrich). The bath was held at 73 °C to maintain the wax in a liquid state for spotting. The wax spotting process involved dipping the spotting tip inside the bath to collect a small volume of molten wax on the tip while being retracted from the bath at 12.5 mm/s. The tip was inserted into the microwell at 5 mm/s followed by a dwell time of 6 s after contacting the well surface to allow the wax to re-melt and deposit on top of the reagent spot before being retracting at 12.5 mm/s.

### C. Isothermal amplification

Isothermal amplification by RCA was performed using a custom benchtop system capable of precise temperature control.<sup>49</sup> The RCA reaction was conducted using purified oligomer sequences designed using NUPACK software<sup>50</sup> and synthesized commercially (Integrated DNA Technologies, Coralville, IL) with the following sequences:

PLP100Phos (template): 5'-Phos/CGT TTT TTC TGT TAT ACT CGA ATG CTA AGA TGA ACA TAT TAA ATG GAG ACT AAG TAA AAC TGA GAC TGA TGT CCT ATG GTC ATA AAT AAC TTC TAT A-3'

GeneSplint2 (splint): 5'-TAT GCT ATC TCA GAA AAA ACG TAT AGA AGT TCA ACT GTC TAG-3'

ProbePhos (probe): 5'-CGA ATG CTA AGA TGA ACA TAT TAA ATG GAG/Phos/-3'

PrimerTail2 (primer/target): 5'-TTT TTT ATG ACC ATA GGA CAT CAG TC-3'

The RCA sample mix consisted of ligation reaction mix, master mix, and primers combined in a volume ratio of 10:4:1, respectively. The primers were mixed with the spotting buffer matrix as described in the pin spotting section to yield final concentrations of 20, 40, or 60 nM when dissolved in the microwell volume after sample infusion. The RCA sample mix was prepared

by first combining the components of the ligation reaction mix together and allowing it to rest for 15 min at room temperature to complete the ligation reaction. The ligation reaction mix consisted of 100 nM PLP 100 (IDT), 1× NEbuffer 2 (New England Biolabs; NEB, Ipswich, MA), 1 mM ATP (P0765L, NEB), 100 nM Gene Splint 2 (IDT), and 10 U/μl T4 DNA ligase (NEB). Simultaneously, the master mix containing 1× NEbuffer 2 (NEB), 2.4 mM dNTPs (NEB), 66.67 U/ml vent (exo-) (M0257S, NEB), 0.9 μM probe phos (IDT), and 3× SYBR dye (S7563, Thermo Fisher Scientific, Waltham, MA) was prepared. Upon the completion of the ligation reaction, the ligation mix was added to the master mix. This was followed by the addition of 0.75% (v/v) PEG (average MW 10 kDa, Sigma Aldrich) for dynamic surface passivation and 0.5% (v/v) Triton X-100 (Sigma Aldrich) to the sample mix.<sup>48</sup> Finally, the sample was infused into the 2D array, followed by discretization using silicone oil with 0.05% (v/v) Span 80 (Sigma Aldrich). The filling and discretization steps were carried out by placing the chip on ice to prevent early enzymatic activity. The RCA reaction was continuously monitored by capturing fluorescence images at an interval of 10 s followed by the final image analysis using ImageJ software (National Institutes of Health, Bethesda, MD) at the end of the reaction. Identical experiments performed in a benchtop thermal cycler (MJ Mini Opticon, Bio-Rad, Hercules, CA) using the same reagents (without PEG) and reaction conditions served as a reference for the evaluation of on-chip assay performance.

## III. RESULTS AND DISCUSSION

### A. Reagent deposition

Reagent deposition was carried out in cubic microwells patterned by CNC micromilling, with edge dimensions ranging from 400 μm to 1.5 mm. During initial experiments, solutions spotted onto the milled surfaces were observed to spread due to surface roughness, resulting in larger spot diameters with high variability. To prevent unwanted spreading, all well surfaces were solvent polished to reduce the surface roughness prior to testing.

Following microwell patterning, reagents were deposited into individual wells using the pin spotting method shown in Fig. 3(a). Before spotting, the reagent solution was loaded into the pin by immersing the tip in the reagent reservoir for 1 min, allowing the solution to fill the internal pin volume by capillary action. Based on the pin geometry, interfacial properties of the spotting buffer, and submersion time, the sample volume aspirated into the pin is estimated using the Washburn equation<sup>51</sup> to be approximately 15 nl.

Due to the small well dimensions, the spotting process requires precise alignment of the spotting pin relative to the microwell array. To this end, the spotting tool stage was modified with a pair of alignment pins, and each array chip was fabricated with matching holes to establish gross axial and rotational positioning of the array on the stage. Similarly, a fixed alignment mark on the stage is used to manually position the pin at the start of each spotting process. Finally, to ensure precise ( $\pm 50 \mu\text{m}$ ) alignment for all wells within the full array, several test spots are deposited and observed *in situ* using a portable USB microscope before initiating deposition.

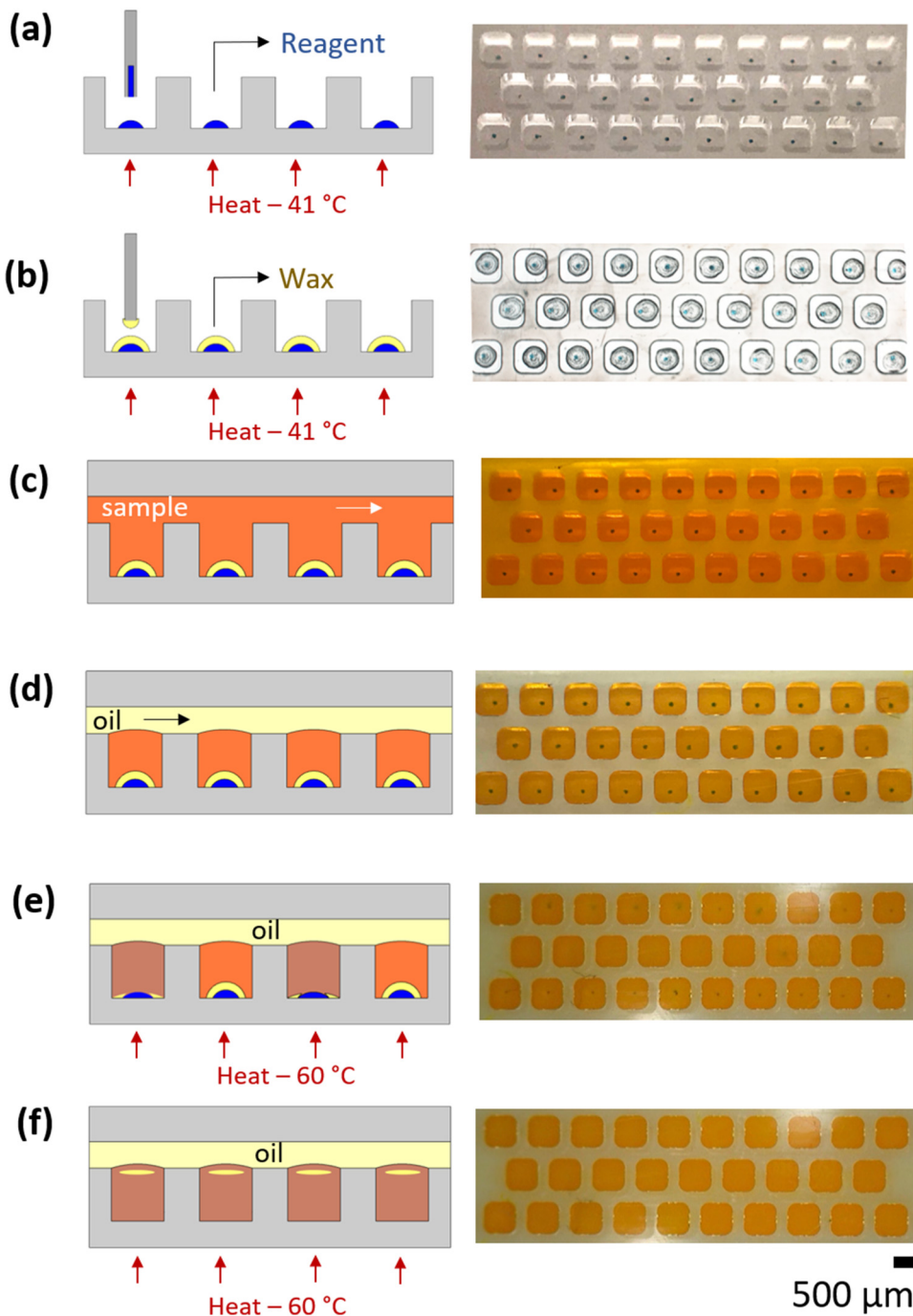


**FIG. 3.** Operation of 2D microwell array with integrated reagents: schematic side views of arrays (left) and the corresponding experimental images (right) at different operating points (a) reagent deposition inside microwells followed by drying, (b) deposition of modified paraffin using the "pick-and-place" method, (c) sample filling, (d) sample discretization during oil introduction, and [(e) and (f)] temperature-controlled release of encapsulated reagents. Molten paraffin floats on top.

Spot size and volume uniformity are critical to ensure the deposition of consistent reagent amounts. Viscosity and surface tension of the spotting buffer can both impact deposition performance. While low viscosity can result in rapid and uncontrollable spreading of deposited spots, excessively high viscosity prevents the flow of reagent solution from the tip onto the substrate and can

cause tip clogging. We found that the combined addition of 10% (v/v) glycerol and 20% (w/w) PEG (average MW 20 kDa) to the spotting buffer provided a suitable viscosity for reliable spotting onto the thermoplastic well surfaces. In addition to modifying the viscosity of the spotted reagent solution, glycerol also helps to slow evaporation during spotting,<sup>37</sup> while PEG is known to be beneficial

for stable long-term storage of dried reagents.<sup>52</sup> Surface tension of the spotting buffer was also adjusted by adding 0.1% (v/v) TritonX-100 surfactant. The surfactant served to promote droplet break off from the spotting tip during deposition, resulting in more uniform anchoring of the spotted droplets. Using the optimized spotting buffer composition, consistent contact deposition of picoliter-scale aqueous sample was achieved within the microwells. When using the custom spotting pins with an inner diameter of 60  $\mu\text{m}$ , an average spot diameter of 95  $\mu\text{m}$  was achieved with a relative standard deviation of 5%. With a measured sessile contact angle of 10° on the hydrophilic-modified COP surface, the mean volume for the deposited spots is estimated to be 40 pl with a standard deviation of 6 pl. For applications requiring larger reagent volumes, multiple spotting events may be performed inside a single microwell. Consistent reagent deposition was achieved up to a maximum spotting frequency of 1.3 Hz limited only by the speed of the motorized stages used in this work.

### B. Reagent encapsulation using wax deposition and controlled release

As the deposited reagents are water soluble, they must be encapsulated to prevent rehydration and dissolution during sample filling and avoid reagent loss or transfer between different microwells. To this end, several polysaccharides (sucrose, PEG, dextran, and gelatin) were evaluated for their efficacy in reagent encapsulation (see Table S1 in the [supplementary material](#)). However, these polysaccharides failed to protect the reagent from rehydration beyond a few seconds during active flow through the chip due to the high solubility of the encapsulants. In contrast, a thin cap of soft paraffin wax was able to encapsulate the reagents indefinitely before a temperature trigger was provided for the controlled release of the reagents. The petrolatum wax consists of a mixture of paraffins with varying molecular weight,<sup>53</sup> and due to its low melting temperature of 37 °C, the wax was readily transferred using the spotting technique. Furthermore, the use of paraffin wax in reaction mixtures for nucleic acid amplification has been reported to improve both amplification performance and long-term reagent stability,<sup>54</sup> and paraffin encapsulation has also been successfully used to avoid the need for a hot start in PCRs,<sup>55,56</sup> making it an excellent choice for reagent encapsulation and controlled release in the present work.

While paraffin wax offers a route to effective reagent encapsulation, the material is highly hydrophobic. As a result, the paraffin spots can serve as hydrophobic barriers that prevent wetting by infused samples. In our initial experiments, this behavior was found to result in routine trapping of air bubbles inside the microwells during sample filling, particularly for wells with side lengths smaller than 1 mm. This issue was circumvented by incorporating a surfactant in the paraffin matrix to increase the wax surface hydrophilicity. The choice of surfactant was driven by consideration of the hydrophilic–lipophilic balance (HLB), defined as the ratio of hydrophilic to hydrophobic regions within the surfactant molecule scaled by a factor of 20; surfactants with HLB < 10 possess more hydrophobic regions and are soluble in the wax phase, while surfactants with HLB > 10 are water soluble.<sup>57</sup> Span 20 was chosen as the surfactant due to its HLB of 8.6,<sup>57</sup> ensuring acceptable wax

solubility while presenting hydrophilic regions on the wax surface. In addition to modifying the wax, surfactant was also added to the sample solution prior to filling the microwells. Several surfactants were evaluated for this purpose, as listed in Table S2 in the [supplementary material](#). While the addition of surfactant to either the wax phase or the sample phase alone successfully reduced the sessile contact of water on the wax surface, the contact angle reduction for either case did not provide adequate wetting to eliminate bubbles during filling. However, the addition of surfactants with moderate HLB values to both the wax and sample phases resulted in a significant contact angle reduction for bubble-free filling within the microwell system containing the wax-encapsulated reagents. The reduction in the contact angle for the wax surface served to introduce asymmetry in the contact angles between the channel and microwell surfaces, thereby promoting the preferential wetting of well side and aiding in the bubble-free filling.<sup>48</sup> Notably, the addition of TritonX-100 (HLB 13.4) to the sample phase resulted in a significantly greater contact angle reduction in the hydrophilic-modified wax when compared to Tween-40 (HLB 15.6) in the sample phase, presumably due to the greater number of lipophilic regions enhancing preferential wetting of the wax surface.

Surfactant-modified wax was deposited into the microwells using a pick-and-place method [Fig. 3(b)]. Unlike reagent deposition, where the fluid is aspirated into the capillary tip to enable multiple sequential spotting events, the high wax viscosity, the low wax wetting of the needle surface, and the lack of temperature control in the needle make wax aspiration impractical. Instead, the spotting tip was dipped into a molten wax bath held at 73 °C prior to each encapsulation step, allowing the needle to retain a small volume of wax on its surface for transfer to a microwell. The wax cools during transfer but melts upon contact with the microwell substrate, which is held at 41 °C during the spotting process simultaneously, transferring a consistent volume of wax from the needle to the dried reagent spot for encapsulation. The volume of wax deposited was observed to be a function of the retraction speed of the pin from the molten wax bath, the dwell time of the pin during deposition, and the substrate temperature. The amount of wax retained on the pin was inversely proportional to the speed at which the pin was retracted from the molten wax bath during the wax uptake. The amount of wax deposited on the substrate was directly proportional to the dwell time and substrate temperature, with higher temperature resulting in greater spreading of the wax spot. For the selected operational parameters, the technique resulted in wax spots with an average diameter of 275  $\mu\text{m}$  with a relative standard deviation of 4.4%. The surfactant-modified wax exhibited a sessile contact angle of 20° on the hydrophilic-modified COP substrate, yielding an estimated wax volume of 1.98 nl.

Upon the completion of the reagent and wax deposition steps, the devices were solvent bonded. No visual changes to the deposited wax-encapsulated reagent spots were observed during the bonding process. After bonding, the sample was perfused through the main channel to fill the wells [Fig. 3(c)], followed by oil discretization [Fig. 3(d)]. Because the devices employed in this work follow validated design rules for thermoplastic 2D microwell arrays,<sup>48</sup> the filling and discretization processes are insensitive to

flow rate. After discretization, the chips were placed on a thermal stage followed by the temperature-controlled release of encapsulated reagents [Figs. 3(e) and 3(f)] at 60 °C. Heating the device beyond the paraffin melting point allowed the wax to melt and migrate away from the center of the microwell, thereby allowing the spotted reagent to diffuse into the discretized aqueous sample phase in the microwell. Because the soft paraffin used in this work has a low density of approximately 0.9 g/cm,<sup>3,53</sup> the wax rises to the top of the wells during the reagent release process.

### C. Multiplexed reagent integration

Simultaneous detection of multiple analytes from a single sample (multiplexing) can be very useful in a resource-limited point-of-care setting as it can minimize sample consumption and keep the test costs low. In such a scenario where the costs and portability are more important than the degree of multiplexing and throughput, the pin spotting approach can provide a cost effecting solution with excellent spatial control for the patterning of different reagents in individual microwells for multiplexed analysis. This is illustrated in Fig. 5 where two reagents (represented by green and yellow food dyes) are spotted in different microwells [Fig. 4(a)] and encapsulated by hydrophilic-modified paraffin [Fig. 4(b)]. Upon sample filling, discretization, and controlled release of the dyes [Fig. 4(c)], no crosstalk between the microwells was observed, thereby establishing the potential for highly multiplexed nucleic acid testing with integrated reagents.

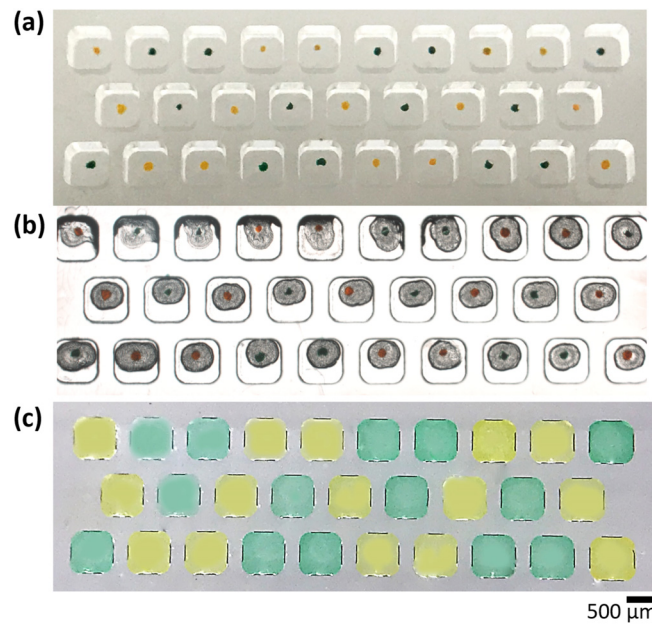


**FIG. 4.** (a) Multi-reagent spotting in cubic microwells ( $L = 800 \mu\text{m}$ ) with two sample solutions (green and yellow dyes). (b) Encapsulation with paraffin spotting and (c) temperature-controlled release of encapsulated reagents.

### D. RCA in 2D microwell array with integrated reagents

When coupled with microfluidic technology, diagnostics based on nucleic acid amplification can enable rapid and multiplexed near-patient testing.<sup>58</sup> While polymerase chain reaction (PCR) has been the preferred option for highly reliable nucleic acid amplification, it requires precisely controlled thermal cycling conditions, which can limit its use in many environments. As an alternative to PCR, isothermal amplification is an emerging diagnostic technique for point-of-care analysis. Isothermal amplification by RCA is particularly attractive due to its simplicity, high amplification efficiency, high specificity, and scope of sequencing for the amplified products.<sup>58–60</sup> Furthermore, RCA is an attractive option for on-chip multiplexed assays, especially with integrated reagents such as the microarrays, since the amplified product remains linked to the deposited primer, thereby localizing the amplified signal and avoiding crosstalk.<sup>61,62</sup>

While there have been limited demonstrations of RCA on the microfluidic chip using primer immobilization on beads for reagent integration,<sup>63</sup> we are particularly interested in validating the pin spotting method as suitable reagent integration in 2D microwell arrays using a high sample concentration. Specifically, we intend to assess key functionalities of this system such as reliable filling of RCA samples in these microwells having the hydrophilic-modified paraffin, proper reagent encapsulation during filling and discretization, and temperature-controlled release of reagents followed by amplification without any inhibition from the paraffin.

As initial steps, determination of appropriate reagent concentration for optimum sensitivity and dynamic range of detection is a key step in assay optimization. Typically, this would involve multiple experiments, each with varying reagent concentration and would also entail substantial sample volume consumption with each iteration. However, such iterations can be reduced significantly by utilizing the multiple spotting capability of the spotting

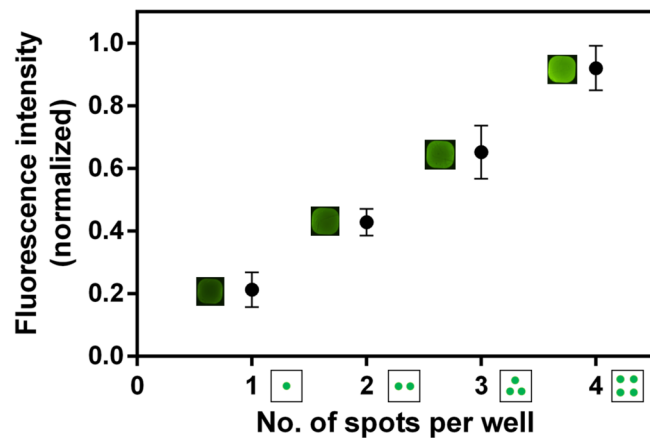


**FIG. 5.** Deposition of multiple sample spots (fluorescein sodium salt) in a single microwell ( $L = 1.5 \text{ mm}$  and  $D = 0.8 \text{ mm}$ ). Fluorescence intensity scales linearly with spot count ( $n = 3$ ; intensity normalized to the peak intensity across all measurements).

technique wherein more than one reagent spot can be deposited inside a microwell resulting in linear increments of reagent concentrations. The linearity of this multiple spotting approach was explored by spotting one, two, three, and four spots of fluorescein sodium salt, respectively, in individual microwells ( $L, W = 1.5\text{ mm}$ ,  $D = 0.8\text{ mm}$ ).  $1.5\mu\text{l}$  of DI water then was added to each microwell, and the resulting fluorescence signal after spot dissolution was measured on a fluorescence microscope. As seen in Fig. 5, there is a linear increase in fluorescence intensity with an increasing number of spots per microwell, indicating the efficacy of this technique for screening various reagent concentrations within a single experiment.

Next, the compatibility of the hydrophilic-modified paraffin was evaluated by performing an on-chip RCA reaction and comparing the assay performance with the conventional method. A solution containing RCA primers was spotted inside cubic microwells with  $800\mu\text{m}$  side lengths and encapsulated with the hydrophilic-modified paraffin. The relatively large microwell dimensions used for this experiment allowed multiple spotting events within each well, allowing the primer concentration to be varied across the array by changing the number of spots. In order to ascertain the appropriate primer concentration, one, two, and three spots of the primers were deposited in the microwells resulting in final estimated primer concentrations of  $20\text{ nM}$  ( $1\times$ ),  $40\text{ nM}$  ( $2\times$ ), and

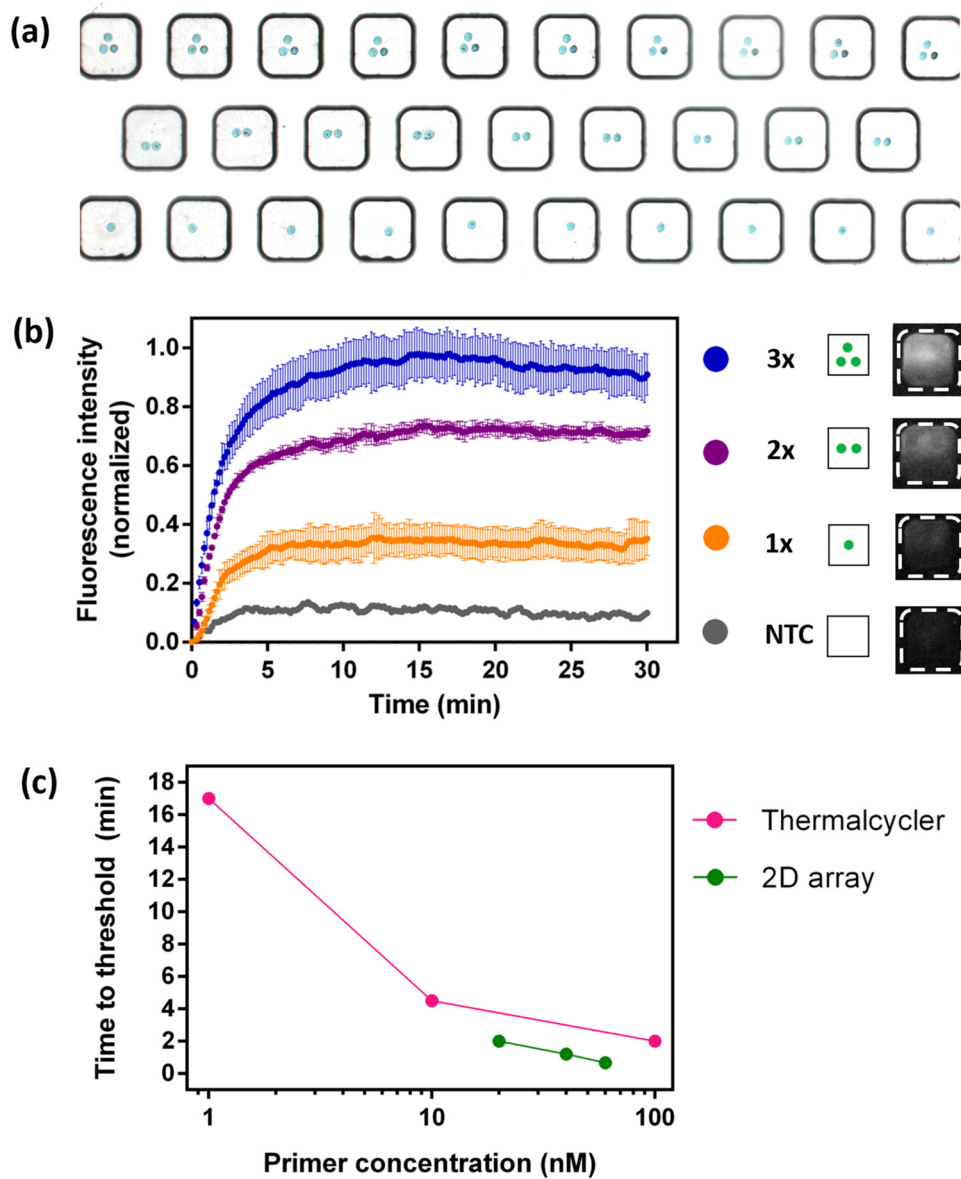


**FIG. 6.** (a) Multiple spotting of primers inside microwells ( $L, W, D = 800\mu\text{m}$ ) (blue dye shown for visualization), (b) RCA in microwells with integrated reagents, where  $1\times$  ( $20\text{ nM}$ ),  $2\times$  ( $40\text{ nM}$ ), and  $3\times$  ( $60\text{ nM}$ ) correspond to one, two, and three reagent spot(s) per microwell, respectively, and NTC is no target control. Data normalized to maximum fluorescence intensity at  $60\text{ nM}$  primer concentration ( $n = 5$  for  $1\times$ ,  $2\times$  each and  $n = 3$  for  $3\times$  primer concentration, error bars correspond to 95% confidence interval). (c) Comparison of RCA time to the threshold between the microfluidic 2D array platform and a conventional thermal cycler.

60 nM (3 $\times$ ), respectively. Additional wells containing deposited wax spots, but no reagent spots served as no target controls for the reaction. Figure 6(a) shows the image of microwells with multiple dye spots that are representative of primer spots for the RCA reaction. Upon spotting, the device was bonded to channel (H = 400  $\mu$ m) using solvent bonding technique.

The pre-ligated sample containing 100 nM template was then infused into the bonded chip followed by discretization using silicone oil and sealing of access ports. RCA was then performed on the chip that involved a hot start at 80 °C followed by isothermal amplification at 60 °C for 30 min with real-time fluorescence monitoring of individual wells on the benchtop system. An assay with identical reaction conditions and template concentration was performed in vials using a conventional thermal cycler (Fig. S1 in the [supplementary material](#)) and assay performance on both the platforms was assessed by estimating the time to threshold (TTT), defined as the time for the fluorescence signal to reach six standard deviations above the maximum intensity of the no template control (NTC) signal. Overall, on-chip RCA was found to yield a faster time to threshold (TTT) at a given primer concentration when compared with the conventional benchtop assay [Fig. 6(c)]. These results confirm the compatibility of the reagent integration technique, including the use of hydrophilic-modified wax for reagent encapsulation and controlled release, with the isothermal RCA assay for on-chip nucleic acid amplification.

#### IV. CONCLUSION

Pin spotting in 2D micowell arrays has been demonstrated as a robust yet simple reagent integration technique for a microfluidic platform. Controlled deposition of reagents and paraffin encapsulant has been demonstrated using a custom spotting pin that employs a small bore cylindrical needle that can be inserted into sub-millimeter well chambers. Bubble-free sample filling is achieved in the microwells with integrated reagents by modifying the surface properties of wax to promote wetting. Reliable reagent encapsulation during sample filling and discretization followed by temperature-controlled release of encapsulated reagents is achieved using this approach. The spotting technique also offers the capability of depositing multiple spots within a single micowell to control the integrated reagent amounts. This approach may also be used to pattern different reagents within individual microwells for multiplexed analysis. While the technique is explored using a single spotting pin in this work, the technique may be readily scaled using a fixed array of low-cost pins for parallel spotting within multiple micowell elements. The functionality of the reagent integration technique in a thermoplastic micowell platform is explored for nucleic acid analysis by performing on-chip RCA, with variable spotting events used to evaluate assay performance across a range of reagent concentrations. The results demonstrate the ability to reduce experimental iterations and sample consumption during assay optimization and support the implementation of disposable nucleic acid diagnostics with seamlessly integrated reagents.

#### SUPPLEMENTARY MATERIAL

See the [supplementary material](#) for a performance summary for various encapsulant materials (Table S1), evaluation of surface

contact angles for different wax and sample surfactant compositions (Table S2), and RCA amplification curves generated using a conventional thermal cycler (Fig. S1).

#### ACKNOWLEDGMENTS

This research work was supported by Canon U.S. Life Sciences Inc., the National Institutes of Health (NIH) through Grant No. R01GM130923, and by the National Science Foundation (NSF) through Grant No. ECCS1609074.

#### DATA AVAILABILITY

The data that support the findings of this study are available within the article and its [supplementary material](#) and from the corresponding author upon reasonable request.

#### REFERENCES

- <sup>1</sup>P. Yager, T. Edwards, E. Fu, K. Helton, K. Nelson, M. R. Tam, and B. H. Weigl, *Nature* **442**, 412 (2006).
- <sup>2</sup>C. M. Pandey, S. Augustine, S. Kumar, S. Kumar, S. Nara, S. Srivastava, and B. D. Malhotra, *Biotechnol. J.* **13**, 1 (2018).
- <sup>3</sup>A. I. Barbosa and N. M. Reis, *Analyst* **142**, 858 (2017).
- <sup>4</sup>E. Primiceri, M. S. Chiriacò, F. M. Notarangelo, A. Crocamo, D. Ardissino, M. Cereda, A. P. Bramanti, M. A. Bianchessi, G. Giannelli, and G. Maruccio, *Sensors* **18**, 3607 (2018).
- <sup>5</sup>C. Dincer, R. Bruch, A. Kling, P. S. Dittrich, and G. A. Urban, *Trends Biotechnol.* **35**, 728 (2017).
- <sup>6</sup>S. Spindel and K. E. Sapsford, *Sensors* **14**, 22313 (2014).
- <sup>7</sup>M. Hitzbleck and E. Delamarche, *Chem. Soc. Rev.* **42**, 8494 (2013).
- <sup>8</sup>R. Bodén, M. Lehto, J. Margell, K. Hjort, and JÄ Schweitz, *J. Micromech. Microeng.* **18**, 075036 (2008).
- <sup>9</sup>S. Smith, R. Sewart, H. Becker, P. Roux, and K. Land, *Microfluid. Nanofluid.* **20**, 1 (2016).
- <sup>10</sup>J. Hoffmann, D. Mark, S. Lutz, R. Zengerle, and F. von Stetten, *Lab Chip* **10**, 1480 (2010).
- <sup>11</sup>J. Kim, D. Byun, M. G. Mauk, and H. H. Bau, *Lab Chip* **9**, 606 (2009).
- <sup>12</sup>J. Song, C. Liu, M. G. Mauk, J. Peng, T. Schoenfeld, and H. H. Bau, *Anal. Chem.* **90**, 1209 (2018).
- <sup>13</sup>W. Liu, A. Warden, J. Sun, G. Shen, and X. Ding, *Biomicrofluidics* **12**, 024109 (2018).
- <sup>14</sup>A. Tupik, G. Rudnitskaya, A. Bulyanitsa, T. Lukashenko, D. Varlamov, and A. Evstratov, *J. Phys. Conf. Ser.* **1124**, 031015 (2018).
- <sup>15</sup>D. Y. Stevens, C. R. Petri, J. L. Osborn, P. Spicar-Mihalic, K. G. McKenzie, and P. Yager, *Lab Chip* **8**, 2038 (2008).
- <sup>16</sup>S. Lutz, P. Weber, M. Focke, B. Faltin, J. Hoffmann, C. Müller, D. Mark, G. Roth, P. Munday, N. Armes, O. Piepenburg, R. Zengerle, and F. Von Stetten, *Lab Chip* **10**, 887 (2010).
- <sup>17</sup>B. A. Rohrman and R. R. Richards-Kortum, *Lab Chip* **12**, 3082 (2012).
- <sup>18</sup>Y. Sun, J. Högberg, T. Christine, L. Florian, L. G. Monsalve, S. Rodriguez, C. Cao, A. Wolff, J. M. Ruano-Lopez, and D. D. Bang, *Lab Chip* **13**, 1509 (2013).
- <sup>19</sup>D. P. Manage, J. Lauzon, A. Atrazev, R. Chavali, R. A. Samuel, B. Chan, Y. C. Morrissey, W. Gordy, A. L. Edwards, K. Larison, S. K. Yanow, J. P. Acker, G. Zahariadis, and L. M. Pilarski, *Lab Chip* **13**, 2576 (2013).
- <sup>20</sup>M. Tijero, R. Díez-Abedo, F. Benito-Lopez, L. Basabe-Desmonts, V. Castro-López, and A. Valero, *Biomicrofluidics* **9**, 044124 (2015).
- <sup>21</sup>C. D. Chin, V. Linder, and S. K. Sia, *Lab Chip* **12**, 2118 (2012).
- <sup>22</sup>I. Barbulovic-Nad, M. Luente, Y. Sun, M. Zhang, A. R. Wheeler, and M. Bussmann, *Crit. Rev. Biotechnol.* **26**, 237 (2006).
- <sup>23</sup>C. Dixit and G. Aguirre, *Microarrays* **3**, 180 (2014).

- <sup>24</sup>B. R. Ringeisen, P. K. Wu, H. Kim, A. Piqué, R. Y. C. Auyeung, H. D. Young, D. B. Chrisey, and D. B. Krizman, *Biotechnol. Prog.* **18**, 1126 (2002).
- <sup>25</sup>A. C. Pease, D. Solas, E. J. Sullivan, M. T. Cronin, C. P. Holmes, and S. P. A. Fodor, *Proc. Natl. Acad. Sci.* **91**, 5022 (1994).
- <sup>26</sup>A. S. Blawas and W. M. Reichert, *Biomaterials* **19**, 595 (1998).
- <sup>27</sup>M. Hengsakul and A. E. G. Cass, *Bioconjug. Chem.* **7**, 249 (1996).
- <sup>28</sup>I. McWilliam, M. Chong Kwan, and D. Hall, *Methods Mol. Biol.* **785**, 345 (2011).
- <sup>29</sup>L. R. Allain, M. Askari, D. L. Stokes, and T. Vo-Dinh, *Fresenius J. Anal. Chem.* **371**, 146 (2001).
- <sup>30</sup>F. G. Tseng, C. J. Kim, and C. M. Ho, *J. Microelectromech. Syst.* **11**, 427 (2002).
- <sup>31</sup>W. Du, L. Li, K. P. Nichols, and R. F. Ismagilov, *Lab Chip* **9**, 2286 (2009).
- <sup>32</sup>V. N. Morozov and T. Y. Morozova, *Anal. Chem.* **71**, 3110 (1999).
- <sup>33</sup>N. V. Avseenko, T. Y. Morozova, F. I. Ataullakhonov, and V. N. Morozov, *Anal. Chem.* **73**, 6047 (2001).
- <sup>34</sup>M. Rahbar, P. N. Nesterenko, B. Paull, and M. Macka, *Anal. Chim. Acta* **1047**, 115 (2019).
- <sup>35</sup>K. Yamada, T. G. Henares, K. Suzuki, and D. Citterio, *Angew. Chem. Int. Ed.* **54**, 5294 (2015).
- <sup>36</sup>G. Arrabito and B. Pignataro, *Anal. Chem.* **84**, 5450 (2012).
- <sup>37</sup>G. MacBeath and S. L. Schreiber, *Science* **289**, 1760 (2000).
- <sup>38</sup>V. Romanov, S. N. Davidoff, A. R. Miles, D. W. Grainger, B. K. Gale, and B. D. Brooks, *Analyst* **139**, 1303 (2014).
- <sup>39</sup>R. S. Kane, S. Takayama, E. Ostuni, D. E. Ingber, and G. M. Whitesides, *Biomaterials* **20**, 2363 (1999).
- <sup>40</sup>J. P. Renault, A. Bernard, A. Bietsch, B. Michel, H. R. Bosshard, E. Delamarche, M. Kreiter, B. Hecht, and U. P. Wild, *J. Phys. Chem. B* **107**, 703 (2003).
- <sup>41</sup>S.-C. S. C. Lin, F. G. F.-G. Tseng, H. M. M. Huang, Y.-F. Chen, Y. C. C. Tsai, C. E. C.-E. Ho, and C. C. C.-C. Chieng, *Sens. Actuators B* **99**, 174 (2004).
- <sup>42</sup>Y. Xia and G. M. Whitesides, *Annu. Rev. Mater. Sci.* **28**, 153 (1998).
- <sup>43</sup>X. M. Zhao, *J. Mater. Chem.* **7**, 1069 (1997).
- <sup>44</sup>A. Sarkar, S. Kolitz, D. A. Lauffenburger, and J. Han, *Nat. Commun.* **5**, 3421 (2014).
- <sup>45</sup>C.-W. Tsao, S. Tao, C.-F. Chen, J. Liu, and D. L. Devoe, *Microfluid. Nanofluidics* **8**, 777–787 (2010).
- <sup>46</sup>C.-W. Tsao, J. Liu, and D. L. Devoe, *J. Micromech. Microeng.* **18**, 025013 (2008).
- <sup>47</sup>G. Fridley, H. Le, E. Fu, and P. Yager, *Lab Chip* **12**, 4321 (2012).
- <sup>48</sup>S. Padmanabhan, J. Y. Han, I. Nanayakkara, K. Tran, P. Ho, N. Mesfin, I. White, and D. L. Devoe, *Biomicrofluidics* **14**, 014113 (2020).
- <sup>49</sup>A. Sposito, V. Hoang, and D. L. DeVoe, *Lab Chip* **16**, 3524 (2016).
- <sup>50</sup>J. N. Zadeh, C. D. Steenberg, J. S. Bois, B. R. Wolfe, M. B. Pierce, A. R. Khan, and R. M. Dirks, *J. Comput. Chem.* **32**, 170 (2011).
- <sup>51</sup>E. W. Washburn, *Phys. Rev.* **17**, 273 (1921).
- <sup>52</sup>A. Ahlford, B. Kjeldsen, J. Reimers, A. Lundmark, M. Romani, A. Wolff, A. C. Syvänen, and M. Brivio, *Analyst* **135**, 2377 (2010).
- <sup>53</sup>A. J. P. van Heugten, J. Landman, A. V. Petukhov, and H. Vromans, *Int. J. Pharm.* **540**, 178 (2018).
- <sup>54</sup>W. Bloch, J. Raymond, and A. R. Read, U.S. patent 5411876A (27 May 1992).
- <sup>55</sup>B. J. Bassom and G. Caetano-Anolles, *Biotechniques* **14**, 30 (1983).
- <sup>56</sup>S. Kaijalainen, P. J. Karhunen, K. Lalu, and K. Lindström, *Nucleic Acids Res.* **21**, 2959 (1993).
- <sup>57</sup>W. C. Griffin, *J. Soc. Cosmet. Chem.* **5**, 249 (1954).
- <sup>58</sup>C. M. Chang, W. H. Chang, C. H. Wang, J. H. Wang, J. D. Mai, and G. Bin Lee, *Lab Chip* **13**, 1225 (2013).
- <sup>59</sup>M. M. Ali, F. Li, Z. Zhang, K. Zhang, D. K. Kang, J. A. Ankrum, X. C. Le, and W. Zhao, *Chem. Soc. Rev.* **43**, 3324 (2014).
- <sup>60</sup>V. V. Demidov and H. Thorne, *Expert Rev. Mol. Diagn.* **2**, 542 (2002).
- <sup>61</sup>G. Nallur, B. S. Chenghua Luo, L. Fang, S. Cooley, V. Dave, J. Lambert, K. Kukanskis, and S. Kingsmore, *Nucleic Acids Res.* **29**, 118e (2001).
- <sup>62</sup>C. C. Chang, C. C. Chen, S. C. Wei, H. H. Lu, Y. H. Liang, and C. W. Lin, *Sensors* **12**, 8319 (2012).
- <sup>63</sup>K. Sato, A. Tachihara, B. Renberg, K. Mawatari, K. Sato, Y. Tanaka, J. Jarvius, M. Nilsson, and T. Kitamori, *Lab Chip* **10**, 1262 (2010).